Experiments and Numerical Simulation of Deflagration-to-Detonation Transition and Detonations in Gaseous and Two-Phase Systems

S. M. Frolov*

Semenov Institute of Chemical Physics, Moscow, Russia

Abstract

Physical principles and problems of controlling deflagration-to-detonation transition and detonation propagation in gaseous and two-phase systems, as well as recent accomplishments of the author's group at Semenov Institute in relevant experimental and numerical studies are outlined. Several examples of detonation devices are discussed, namely (1) the pulse detonation burner operating on natural gas – air mixture, (2) the pulse detonation rocket engine for orbit correction, (3) the air-breathing pulse detonation engine integrated in subsonic and supersonic ramjets, and (4) the pressure gain rotating-detonation combustor designed to replace a conventional combustor in a gas-turbine engine.

1. Introduction

In existing power plants and burning devices chemical energy of fuel is converted into heat and mechanical work by slow burning – deflagration. In addition to deflagration, there is another known combustion mode – detonation. Fuel oxidation in a detonation wave occurs in the mode of self-ignition at high temperature and pressure behind a strong shock wave. Deflagration of air mixtures of hydrocarbon fuels are accompanied with about 1 MW/m^2 heat release per unit area of the reaction front, whereas the heat release in the detonation front is about 4 orders of magnitude higher (~ 10000 MW/m^2). Furthermore, in contrast to the products of slow burning, detonation products have tremendous kinetic energy: the speed of the detonation products is 20–25 times the speed of slow-burning products.

There are two basic schemes of detonation combustion in engines: pulse detonation, when the fuel – oxidizer mixture is burned in the periodic detonation waves traveling along the combustion chamber and continuous detonation, when a detonation wave is continuously rotating in a tangential direction across the annual combustion chamber. Both schemes are considered promising for power engineering as well as air-breathing and rocket propulsion. If, for example, instead of the existing chambers with continuous combustion one applies chambers with pulse or with continuously rotating detonations, these could provide great benefits when used in the energy and propulsion sector due to the energy release with a considerable gain in total pressure and the combined shock wave (mechanical) and thermal effects on the target objects. In view of it, there is a growing interest to the studies of controlled detonations worldwide.

Until now, detonation of fuel–air mixtures has not been widely used in industry, in particular in energy sector, and in propulsion. The main reason for this lies in the problem of detonation initiation. In view of safety concerns, direct initiation of detonation should be immediately excluded from consideration. As regards the deflagration-to-detonation transition (DDT), it is promising only if the problem of ensuring reliable and controllable DDT within a short distance at a small ignition energy can be solved. However the detonability of practical fuel–air mixtures under normal conditions is very low and this problem remained unsolved so far.

2. Specific Objectives

The specific objectives of this paper are to outline the physical principles and problems of controlling DDT and detonation propagation in gaseous and two-phase systems, as well as recent accomplishments of the author's group at Semenov Institute of Chemical Physics in relevant experimental and numerical studies.

3. Results and Discussion

3.1 Physical Principles

The classic mechanism of DDT in a straight smooth tube filled with a homogeneous fuel–oxidizer mixture includes several stages [1, 2], namely, (1) forced mixture ignition with the formation of a laminar flame, (2) progressing increase in the rate of combustion because of the appearance of instabilities and subsequently turbulent flow ahead of the flame front, (3) shock wave formation and amplification ahead of the accelerating flame front, and (4) self-ignition of the shock-compressed mixture in the region between the shock wave and flame front [3] ("explosion in the explosion" [4]) resulting in the formation of an overdriven detonation wave and then (5) self-sustaining Chapman–Jouguet (CJ) detonation. The run-up distance and time of the DDT are known to be largely determined by the first three stages.

Contrary to DDT in premixed gases, DDT in a heterogeneous two-phase mixture is preceded by mixture formation. Despite possible differences in the mechanism of energy release, thermodynamically

* Corresponding author: smfrol@chph.ras.ru

gaseous and heterogeneous detonations are very similar to each other. At similar initial conditions, they have almost same propagation velocities. Moreover, both propagate due to strong coupling between the lead shock wave and chemical energy deposition. In suspensions of very fine hydrocarbon drops in oxygen or air, the observed structure of a heterogeneous detonation wave resembles the structure of the corresponding gaseous detonation. The necessity of ensuring the stability of the "shock wave – reaction zone" complex implies that the reaction completion time in gaseous and heterogeneous detonations should not differ considerably.

Detonation in air mixtures of hydrocarbon fuels requires that the apparent velocity of the turbulent flame front in the laboratory frame of reference be higher than about 1000 m/s [5]. At such a flame front velocity, the shock wave running ahead has a velocity higher than 1300 m/s (the shock wave Mach number is M ~3.8).

In our works [6–10] and reviews [11, 12], a new method for obtaining gaseous or heterogeneous detonation in a straight smooth tube was suggested. Its essence is the forced acceleration of a comparatively weak primary shock wave to intensities sufficient for the onset of a detonation. For this purpose, distributed igniters were mounted along a straight smooth tube. The primary shock wave was generated using either an electric discharge [6–11] or a tube section with a Shchelkin spiral [12, 13] and was accelerated by switching on each ignition source as the wave arrived at the corresponding tube section. In other words, the shock wave was accelerated by providing fast forced mixture ignition in the nearest vicinity of the running shock front.

This technique allowed detonation to be initiated at a distance and in a time much smaller compared with the classic DDT. In experiments [6–11] with detonation initiation, the mismatch between the arrival of the shock wave and gas ignition did not exceed 100 μs. At a larger mismatch, the other conditions being equal, no detonation occurred. Interestingly, the admissible mismatch value is comparable with the characteristic reaction time in the detonation wave at the limit of detonation [14].

The detonation of a stoichiometric propane–air mixture was obtained in a tube 51 mm in diameter at the primary shock wave velocity at a level of 800–1000 m/s (the shock wave Mach number was M ~ 2.4–3.0). Note that, for the formation of a similar shock wave ahead of a flame front, the flame front should be accelerated to an apparent velocity of about 550–750 m/s. This velocity is considerably lower than the velocity of the flame required for the spontaneous DDT (~1000 m/s). It follows that the run-up distance and time of the DDT can be reduced substantially by providing the possibility of forced shock wave acceleration ahead of the flame front; that is, we can then obtain a "fast" DDT. From now on, the fast DDT will be understood as the appearance of detonation in a fuel–air mixture when a turbulent flame is accelerated to a velocity considerably lower than the velocity required for the classic ("slow" [11]) DDT in a straight tube. The new technique for initiating detonation studied in [6–11] was called in [6] "detonation initiation by a running forced ignition pulse."

Let us now turn from DDT in a straight smooth tube to DDT in a tube with regular obstacles [2, 3, 16]. The mechanism of DDT in such tubes is in many respects similar to the classic mechanism described above. There are also important differences. First, the flame is accelerated much faster in a tube with obstacles because of the additional turbulization of a fresh explosive mixture when it flows around obstacles. Secondly, there appear new possibilities for gas ignition. A gas can be self-ignited at the reflection of the shock wave from an obstacle or (if obstacles are large) because of mixing of directed jets of hot combustion products with a cold fresh mixture.

The possibility of the local self-ignition of a fresh mixture caused by shock wave reflection from an obstacle suggests an idea [11] that, in DDT in tubes with obstacles, not only the classic scenario, but also the scenario of detonation initiation by a running ignition pulse, however spontaneous rather than forced, is possible. Gas ignition in the vicinity of the shock wave running in front of the flame then occurs because of the self-ignition of the substance compressed by the shock wave reflected from obstacles rather than because of external stimulation of chemical activity. In other words, DDT in tubes with obstacles includes a stage at which fast detonation initiation by a running spontaneous ignition pulse (fast DDT) is possible in principle. As with forced ignition experiments [6–11], the possibility of fast DDT is then determined by the degree to which the time moments of the arrival of the shock wave at one or another tube cross section and gas ignition in the section coincide. In the case under consideration, we must compare the moment of the arrival of the shock wave at an obstacle and the moment of gas self-ignition behind the reflected wave. The latter is, as is well known, characterized by ignition delay.

Ignition delay depends on the composition of the mixture, the intensity of the running shock wave, and the duration of the compression phase in it. Recalling the maximum time mismatch between the arrival of the shock wave and gas ignition (~100 μs) mentioned above, we assume that the admissible self-ignition delay time should be less than 100 μs at the normal reflection of a long-duration shock wave from obstacles. Fast DDT in a stoichiometric propane–air mixture then requires a shock wave running at a velocity of 950–970 m/s (the shock wave Mach number is M ~ 2.8). During DDT, such a wave is formed in front of the flame propagating at a velocity of about 700 m/s. Clearly, the obtained shock wave velocity value is within the range of shock wave velocities used in experiments [6–11] with the initiation of detonation by a running forced ignition pulse. Thus, theoretically, when the velocity of the flame exceeds 700 m/s and the velocity of the shock

wave ahead of the flame front exceeds ~950–970 m/s, fast DDT becomes possible.

Note that the above estimates ignored effects related to explosive mixture expansion in rarefaction waves inevitable in the diffraction of shock waves by obstacles. Inasmuch these effects depend on the shape and positioning of obstacles in a tube, the threshold flame velocity required for fast DDT depends on obstacle configuration. Also, when discussing the DDT in obstructed tubes, we did not pay attention to the fact that obstacles exert different influences on a flame and a shock wave, two major components of the DDT process. A cascade of regular obstacles, which facilitates the rapid acceleration of the flame due to a strong turbulization of the flow, may hinder the spread of the shock wave due to significant momentum losses and thereby impede or preclude the occurrence of DDT. This means that ***fast DDT in fuel–air mixtures can be obtained by a careful selection of the shape and placement of obstacles, providing an optimal matching between the rate of acceleration of the flame and the amplification of the shock wave.*** This idea constitutes the basic principle of the concept of fast DDT, which has been successfully verified for various gas and spray explosive mixtures [15].

Discussed below are several examples of the potential use of controlled fast DDT and detonation propagation in different practical devices for energy and propulsion sectors.

3.2 Natural Gas Fueled Pulse Detonation Burner

According to the available literature data, the sizes of tubes required to realize DDT in mixtures of practical fuels, such as natural gas, with air are, indeed, unacceptably large. For example, Kuznetsov et al. [17, 18] performed a series of experiments on DDT in methane–air mixtures of different compositions in straight closed tubes of different diameter equipped with regular orifice plates with a blockage ratio of 0.3–0.6 installed at regular intervals equal to the tube diameter. Under normal conditions, DDT was observed only in tubes of diameter 520 and 174 mm, with the minimum distances from the ignition source to the point of detonation onset being 15–17 m and 6–8 m, respectively [18]. It is noteworthy that, in a tube with a diameter of 121 mm, DDT was observed only at an elevated initial pressure (2 atm or higher) at a distance of $L_{DDT} > 4–5$ m. However, the results of Kuznetsov et al. [18] contradict the data of Vasiliev [19], who observed DDT to occur within a very short distance, $L_{DDT} = 2.5–3$ m, in a stoichiometric methane–air mixture under normal conditions in a closed tube of diameter 100 mm equipped with special-shape obstacles (protected by a patent). In addition, the results of Kuznetsov et al. [18] contradict the known fact that the limiting diameter of a smooth tube in which a methane–air mixture can detonate under normal conditions is close to 100 mm. For example, recently Frolov et al. [20] successfully initiated a detonation in a stoichiometric methane–air mixture under normal conditions in a tube with a

Fig. 1. Pulse detonation burner.

diameter of 94 mm at a relatively low Mach number, $M = 3.3$, of the shock wave during its diffraction on a single obstacle of special shape, a convergent-divergent nozzle.

The results of Vasiliev [19] and Frolov et al. [20] suggest that the reason for this contradiction lies in the different influences of differently-shaped obstacles on a flame and a shock wave, two major components of the DDT process. In 2010, we have applied the concept of fast DDT [15] to develop and test the experimental model of Pulse-Detonation Burner (PDB) fueled by natural gas – a prototype of industrial burners of new generation combining the shock-wave (mechanical and convective) and thermal impact on target objects [21] at very low NOx emissions [22]. The most important result of [21] is the proof of feasibility of cyclic DDT with the detonation run-up distance of 2.5–3 m in the tube of near-limit diameter (94 mm) with an open end at separate feed of natural gas and air with a relatively low ignition energy (~1 J). The problem of fast DDT was solved by careful selection of the shape and placement of obstacles, providing optimum adaptation of the rates of flame acceleration and shock wave amplification. The PDB model [21, 22] operated with a low frequency of 0.03 Hz due to low supply velocities of natural gas and air (~0.5–1.0 m/s).

Here, we describe the results obtained in the modified PDB model operating at a considerably higher frequency (up to 2 Hz) due to increase in the supply velocity of natural gas and air (up to 10–12 m/s). Reported below are the results of experiments demonstrating the PDB operation process in terms of cyclic detonation initiation via fast DDT. The results provide a basis for further work aimed at increasing the operation frequency and thermal power of PDBs for different industrial (metallurgy, chemical engineering, waste incineration, etc.) and propulsion applications.

The PDB (Fig. 1) consists of two coupled sections: the mixing/ignition section (MIS) with a spark-ignition source (ignition energy less than 1 J; 2 to 4 standard automobile spark plugs) and the burner duct – a straight tube of 150 mm in diameter and 5.5 m long with obstacles of special shape and placement. The main

principles of obstacle shaping and placement are disclosed in patents [23–25]. The shape, pitch, and blockage ratio of obstacles vary with distance from the ignition source. ***This variation first ensures the fastest possible flame acceleration for generating a sufficiently strong shock wave, and then it ensures the fastest possible transition of this shock wave to a detonation due to its focusing at shaped obstacles of low hydrodynamic drag.*** The end of the burner duct is open to the atmosphere. The last three sections of the tube of 2 m total length, adjacent to the open end of the burner duct are made smooth, i.e. there are no obstacles inside.

The operation cycle of the PDB consists of several stages. Their duration is controlled by a digital controller. Both components of the mixture are delivered in MIS through separate lines equipped with check valves. Natural gas containing 98.9% methane (according to certificate) is fed into the burner through the receiver 200 L in volume at overpressure of 0.3 atm connected to the natural gas manifold via a control valve. Ambient air is fed into the PDB with a vortex blower, which provides airflow up to 0.5 m^3/s. In the first stage the PDB is filled with a mixture of natural gas and air at a (currently) maximum fill rate of about 10–12 m/s (fill time 350–450 ms). When filling the PDB with a combustible mixture the mass flow rates of components are adjusted to ensure that mixture composition is close to stoichiometric (mixture composition is checked by chromatographic analysis of probes taken in several tube sections), i.e. the volume concentration of methane is $(9.5 \pm 0.3)\%$. To avoid leakage of fresh mixture through the open end of the burner duct the PDB is filled only partly with the mixture. The digital controller sets the time of filling the burner duct to avoid leakage through its open end even for the most undesired condition of DDT failure: a mixture is completely burned in both the detonation and deflagration modes.

In the second stage, after shutoff of natural gas supply (with a fast-acting valve) multipoint fuel-air mixture ignition is triggered in MIS followed by automatic stopping of air supply, fast flame acceleration in the burner duct and DDT at a distance of ~3.5 m from the ignition source for ~20 ms after ignition.

In the third stage, the shock wave exits from the duct open end followed by the outflow of the detonation products. If one assumes that the average velocity of the bulk of the combustion products through the open end of the burner duct in the atmosphere is close to the characteristic sound velocity in the combustion products (~1000 m/s), the duration of emptying the duct from the products will be several tens of milliseconds, i.e. the time interval comparable to the total time of mixture burnout via DDT.

In the fourth stage, the PDB is first purged with air over ~50–100 ms and then the supply of natural gas and air is resumed, thus the next cycle starts.

The maximum pulse frequency in our conditions was about 2 Hz. Duration of our experiments while working with detonation frequency of (1.8 ± 0.1) Hz reached 300 s.

In general, the following parameters of the process were recorded in the course of experiment: pressure in MIS (using low-frequency KARAT-DI60 pressure sensor); pressure in different sections of burner duct (using 11 high-frequency PCB113A23 pressure sensors); ionization current between the electrodes of 4 ionization probes installed in the same duct sections as pressure sensors 8 to 11 located in a smooth section of the duct; temperature of PDB structural elements using 6 thermocouples of type K; and temperature of the heat target installed at a distance of 100 mm from the PDB open end using 2 thermocouples of type K. The heat target of 11 kg mass (steel) had a shape of disk inclined to the burner axis at an angle of 45^o. Signals from the sensors, probes, and thermocouples came through amplifiers and analog-to-digital converter (sampling frequency of 1 MHz) to a personal computer. During long-duration experiments only signals of thermocouples and signals of ionization probes used to monitor the speed of the reaction front were recorded. After the termination of long-duration experiments a thermal imaging camera (TESTO) was used to additionally control the final temperature of different parts of PDB.

The average velocity of the shock wave front at each measuring segment between adjacent pressure sensors in the burner duct was determined by the distance between the sensors and the time interval between the arrival of the shock wave at the sensors in the pressure records. The relative error in the average detonation velocity is estimated as a sum of relative measuring errors of distance between the pressure sensors (0.4%) and shock arrival times at neighboring sensors (1.6%) and is equal to 2%.

Detonation in the experiments was identified by four characteristics: (1) highest speed (1600 m/s and above) of a quasi-stationary shock wave in a smooth section of the burner duct, (2) the level of pressure (30 atm and above) registered by PCB sensors (the relative measuring error of PCB sensor is 5% at 100^oC), (3) characteristic footprints on 1-meter long smoked foil (spin pitch 400–500 mm), inserted into the open end of the burner duct, and (4) matching records of pressure sensors and ionization probes installed in one section of the duct (“simultaneous” sharp deviation of both records).

The most important result of this work is the proof of feasibility of fast cyclic DDT with a frequency of up to ~2 Hz in a high-speed flow (10–12 m/s) of natural gas – air mixture. It is experimentally proved that the use of obstacles of special shape and placement in the burner duct can provide reliable cyclic DDT at a distance of ~3.5 m for about 20 ms after ignition.

Figure 2 shows the pressure records in a single PDB cycle with the fast cyclic DDT with cycle frequency of (1.8 ± 0.1) Hz and a photograph of the smoked foil footprint in a single shot with the fast DDT, and Fig. 3 compares the signals of pressure sensor 9 and the

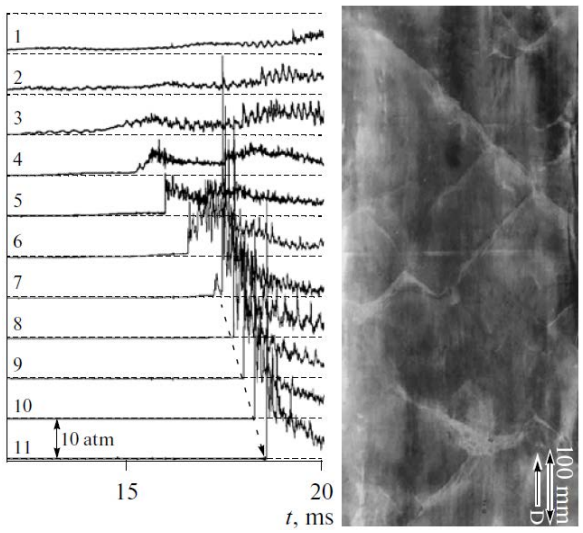

Fig. 2. Oscillograms of the pressure measured by sensors 1–11 during one of the cycles of an experiment with fast cyclic DDT (left) and a photograph of the smoked-foil pattern of the detonation wave (right). The dashed line shows the trajectory of the detonation wave.

ionization probe, installed in the same section of the burner duct, at cyclic PDC operation with cycle frequency of (1.8 ± 0.1) Hz. The numbering corresponds to the numbering of the pressure sensors 1 to 11.

It is seen in Fig. 2 that the "explosion in the explosion" occurs between sensors 6 and 7 at ~17.2 ms after ignition. Explosion occurs between shock precursor and flame and leads to overdriven detonation wave running toward the open end of the burner duct and retonation wave traveling towards MIS. In the vicinity of sensor 8 the overdriven detonation catches up with the shock precursor, and the wave of self-sustaining detonation forms which propagates in a quasi-stationary mode towards the end of a smooth section of the duct with a speed of 1600–1700 m/s.

Detonation mode observed in the smooth section of the burner duct should be considered as a near-limit (spinning) regime of self-sustaining detonation. First, the deficit of average detonation velocity of 100–200 m/s relative to the thermodynamic CJ value in a stoichiometric methane–air mixture ($D_{CJ} \approx 1800$ m/s) is consistent with the maximum allowable deficit of the detonation velocity on the limit of propagation in a smooth tube. Second, the structure of the wave corresponds well to the structure of spinning detonation with characteristic weakly damped oscillations of the pressure signal. The oscillation frequency of the signal on the records of pressure sensor 11 is approximately 3.7 kHz (see Fig. 2). This frequency is consistent with the known heuristic rule $s/d \approx 3$, where s is the spin pitch, and d is the tube diameter. Indeed, according to this rule, a spin pitch in the tube 150 mm in diameter should be 450 mm, and with an average speed of spinning detonation of 1600–1700 m/s the characteristic

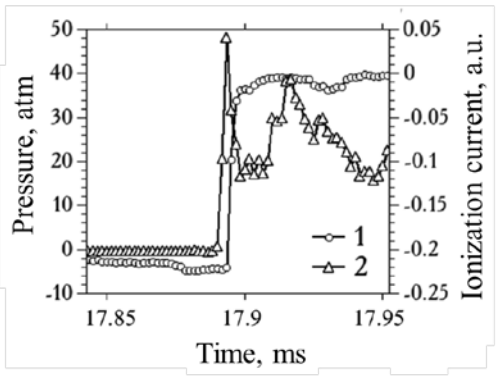

Fig. 3. Records of ionization current between electrodes of ionization probe (curve 1) and pressure at sensor 9 (curve 2) installed in the same section of the burner duct detecting a detonation at cyclic (1.8 ± 0.1) Hz PDC operation.

frequency of the pulsations to be 3.6–3.8 kHz. Third, the smoked foil footprint of the wave in the smooth section of the burner duct in Fig. 2 shows clearly how the overdriven detonation formed by the DDT (with multiple heads in the front) is converted into a spin (inclined blurred line in the upper part of the photo). Pressure peaks in Fig. 2 greatly exceeding the peak value calculated for a plane wave with the CJ parameters also indicate that the detonation propagates in the conventional pulsing mode (multi-headed in the overdriven mode and single-head in the spin mode). In both cases, due to the presence of transverse waves in the reaction zone of the lead shock front the recorded peak pressures are much higher than the CJ pressure. Fourth, Fig. 3 clearly shows that signals of pressure and ionization current sharply deviate from the zero line at apparently the same time – the fact that identifies the detonation. Note that the characteristic response time of both pressure sensor and ionization probe was 3 μs .

Figure 4 shows the pressure records of four sensors 8 to 11 in the smooth section of burner duct in ten consecutive cycles at PDC operation with a frequency of about 1.1 Hz for 10 s. In this experiment, the filling time of PDC with fresh mixture was 420–430 ms. Gradual shift of zero line down for all the pressure sensors is due to thermal effects of the detonation products on the sensors. Figure 4 shows a good repeatability of signals of all sensors, especially the pressure peaks, corresponding to the arrival of detonation. Note that repeatability of signals was good not only within a given run but also from run to run with fixed controller settings.

Black circles in Fig. 5 show the values of detonation velocity obtained between sensors 8 and 9, 9 and 10, 10 and 11 in ten consecutive cycles of Fig. 4. The solid line represents the arithmetic mean of the detonation velocity $\overline{D}$ on the specified measuring segments in ten cycles, and the horizontal dashed line represents the CJ detonation velocity. It can be seen that in this

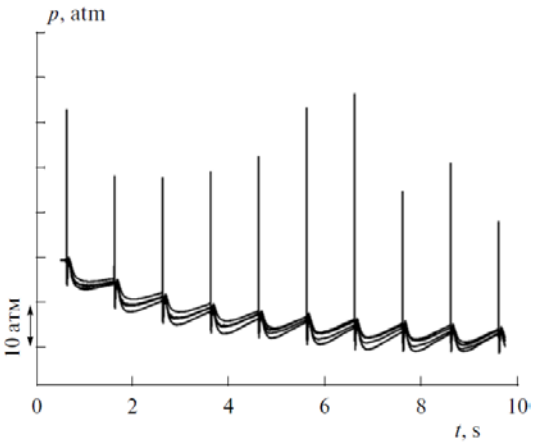

Fig. 4. Oscillograms of the pressure measured by sensors 9 to 11 in the smooth section of the tube during ten consecutive cycles of PDB operation at a frequency of ~1 Hz for 10 s in an experiment with a time of tube filling with fresh mixture of 425 ms.

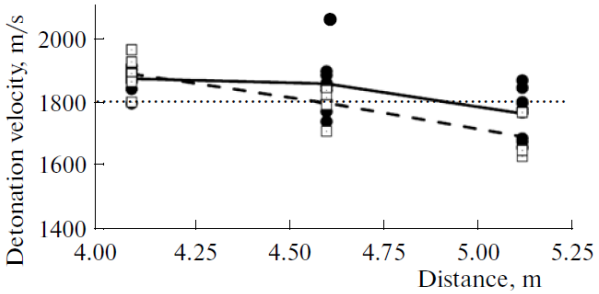

Fig. 5. Experimental value of the velocity D at the measurement distances between sensors 8–9, 9–10, and 10–11 in ten consecutive cycles in two experiments: in the experiment specified in Fig. 4 (closed circles) and in experiment with shorter filling time (open squares). The solid and dashed lines represent the arithmetic mean of the detonation velocity in the respective experiments. The dotted line is the CJ detonation velocity.

experiment detonation in a smooth section of the burner duct (between sensors 8 to 10) first propagates in the overdriven (in average) mode with a degree of overdrive 3–4% ($\overline{D} = (1.03-1.04)D_{CJ}$), and in the last measuring segment (between sensors 10 and 11) with an average velocity of just under D_{CJ} ($\overline{D} \approx 0.98D_{CJ}$). Overdriven detonation is known to form in the process of DDT [1–4]. The average detonation velocity decreases at the last measuring segment due to two reasons. First, there is a natural weakening of overdriven detonation caused by the rarefaction wave from the combustion products. Secondly, due to the partial filling of the burner duct with combustible mixture its composition at the end of the duct is different from that all over the duct (a mixture can be partly diluted with purging air).

For comparison, white squares in Fig. 5 show the values of shock wave velocity between pressure sensors 8 and 9, 9 and 10, 10 and 11 in another experiment with ten consecutive cycles, but with a fill time of 370–380 ms. Reducing the fill time by ~50 ms as compared with the previous example led to the observation of the overdriven detonation mode only between sensors 8 and 9, whereas between sensors 9 and 10 the average detonation velocity in ten cycles decreased to 1800 m/s and further to 1700 m/s between sensors 10 and 11.

3.3 Pulse Detonation Rocket Engine for Orbit Correction

At present, the possibilities of improving the existing types of liquid rocket engines (LRE) for space transportation systems are almost completely exhausted. Hopes for a qualitative leap in the development of outer space engines are pinned on the development and introduction of fundamentally new rocket engines based on pulse or continuous detonation combustion. In pulse detonation rocket engines (PDREs), the fuel components, periodically injected into the combustion chamber, chemically react in periodically initiated detonation waves.

A promising application for PDREs, more specifically, micro-PDREs, is to correct the position and to execute orbital maneuvering of satellites [26]. It is expected that, due to a high thermodynamic efficiency of detonation combustion cycle [27], digitally calibrated bits of thrust, and controlled repetition frequency of detonation pulses, such micro-PDREs will surpass the existing analogues not only in design (manufacturability, ease of construction, etc.) and performance (reliability, cyclic stability, etc.), but also in terms of specific propulsion characteristics (specific impulse, specific mass, etc.). The design of micro-PDREs has not yet been determined.

The aim of the work outlined in this Section is to try to shape the future design of micro-PDREs for spacecraft control systems on the basis of a laboratory realization of a calibrated high-frequency pulse-detonation cycle in liquid hydrocarbon fuel – gaseous oxygen sprays in short tubes of small diameter. In the course of the work, we assembled an experimental setup with systems of fuel and oxidizer supply, ignition, power supply, diagnostics, monitoring of combustible gases, emergency security, and digital control. In addition, we developed and tested a pulse ignition unit (PIU) operating both in a single-pulse mode and in a repetition mode with variable pulse frequency and constructed and tested a high-frequency demonstrator of the operation process of micro-PDREs (Fig. 6).

The demonstrator consisted of a PIU and a detonation tube attached to it. The housing of the PIU was made of brass. Gaseous oxygen was supplied into a cooling jacket with internal ribs. The channels of the heat exchanger were arranged in such a way as to make the high-speed oxygen flow cross the jet of liquid fuel (*n*-heptane, supplied by a conventional automobile fuel injector) and direct the fuel into the nozzle hole that connects the feed system with the combustion chamber of the PIU.

The PIU combustion chamber had a complex shape,

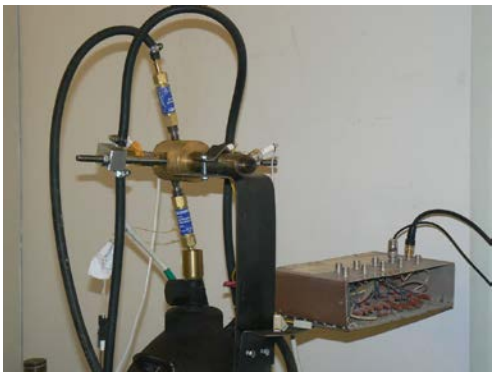

Fig. 6. General view of micro-PDRE.

with divergent-convergent areas. ***This shape ensured fast flame acceleration leading to shock formation and further shock-to-detonation transition in a specially profiled focusing nozzle.*** The principles of nozzle shaping are disclosed in patent [24] and discussed in [28–30, 20]. In [28], it was experimentally shown that installation of a focusing nozzle in a tube ensures the shock-to-detonation transition in a stoichiometric propane–air mixture at a shock wave velocity at the nozzle inlet above 680 ± 20 m/s, which approximately corresponds to a Mach number of 2.

The PIU combustion chamber had holes in the walls for standard automotive spark plugs or screw caps. The steel detonation tube, 8 mm in diameter and 120 mm in length, was joined to the nozzle of the combustion chamber of the PIU via a threaded connection. Along the detonation tube, screw holes for accommodating ionization probes were made 100 mm apart.

In the firing tests, we used 2 ionization probes. The probe was an isolated steel rod fastened in a threaded bushing. During measurements, the rod was deepened into the tube by at least a third of its inner diameter. A DC voltage, from +100 to +200 V was applied to the rod. In the presence of negative charges in medium, an electric signal appeared in the circuit of the probe, which was fed into an USB-300 analog-to-digital converter (with an acquisition time of 0.3 μs) and then into a personal computer. The time constant of the probe was essentially dependent on the conductivity of the medium, typically less than 3 μs and ~1 ms, for detonation and deflagration, respectively.

The operation of all systems of the micro-PDRE demonstrator, including the emergency cutoff of the combustible mixture components, was managed by a digital controller. During the firing tests, the fuel pump ran continuously. At some predetermined time t_1, the digital controller actuated the solenoid valve of the injector, and the fuel started flowing into the combustion chamber of the PIU. Later, at time t_2, the digital controller actuated the ignition coil circuit and, then, at time t_3, produced a fuel cutoff signal. At time t_4, the power supply of the plugs was switched off. The supply of fuel through the injector was renewed at time t_5. Oxygen was fed into the PIU continuously. The main settings of the PIU were the fuel supply duration ($\Delta t_{1–3}$= $t_3 - t_1$), ignition advance ($\Delta t_{2–3} = t_3 - t_2$), spark discharge duration ($\Delta t_{2–4} = t_4 - t_2$), duration of blow-through of the PIU with oxygen ($\Delta t_{4–5} = t_5 - t_4$), and the pressure of oxygen supply.

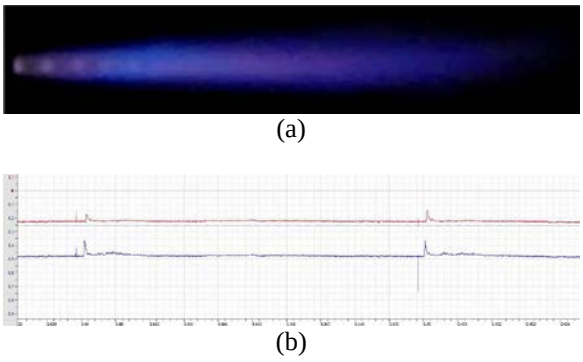

(a)

(b)

Fig. 7. PDRE exhaust plume (a) and voltage signals of two ionization probes (b) at operation frequency of 100 Hz.

The schedule of firing tests of the micro-PDRE demonstrator included tests in single-pulse and repetition modes at different ambient conditions up to vacuum. In the course of tests, the settings of the PIU were varied, exhaust plume was filmed, and signals from the ionization probes were recorded. As a result, we determined the conditions (the pressure of oxygen supply and durations of the different stages of the operation process) under which DDT occurred in the micro-PDRE demonstrator in both single-pulse and repetition modes. The highest operation frequency of 200 Hz with repeatable detonations was obtained with firing the micro-PDRE in vacuum.

As an example, Fig. 7 shows the exhaust plume and the voltage signals of ionization probes at frequency of 100 Hz in the course of 1-second operation. Upon increasing the temporal resolution of the records (see Fig. 7b), it is possible to calculate the combustion wave velocities over the measurement distance between the probes by the formula $D = \Delta X/\Delta t$, where ΔX is the distance between adjacent probes and Δt is the time interval between the arrivals of the combustion wave to the locations of the probes. An analysis showed that, in all 100 cycles, the combustion wave velocity over the measurement distances was nearly constant, D = 2100–2200 m/s. This value corresponds to the thermodynamic detonation velocity of a n-heptane–oxygen mixture with an oxygen-to-fuel equivalence ratio of 1.5–1.6. In all cycles, the visible flame length was about ~40 detonation tube diameters (see Fig. 7a). The flame pattern was well repeated from pulse to pulse. Thus, the demonstrator provides good repeatability of the shape and duration of pulses, a behavior indicative of reliable periodic DDT in the detonation tube. Note that the developed PIU provides a very fast DDT: detonation-like signal is recorded already by the first ionization probe located at the exit section of the PIU behind the nozzle.

Thus, we developed and tested a high-frequency demonstrator of the operation process of micro-PDREs

operating on liquid fuel to try to shape the future design of a new type of rocket engines for spacecraft control systems. The tests made it possible to determine the conditions under which reliable DDT in both single-pulse and repetition modes took place in the demonstrator.

3.4 Air-Breathing Pulse Detonation Engine Integrated in Subsonic and Supersonic Ramjets

The possibility of increasing the thrust performance of ramjet engines (ramjets) is linked with using pulse detonation combustors (PDCs) [31, 32]. Similar to a PDB described above, the cyclic operation in these combustors involves the following steps: (1) filling the chamber with fuel–air mixture, (2) the ignition of the mixture followed by flame acceleration and DDT, (3) combustion of the mixture in the running detonation wave, and (4) the evacuation of the chamber from the products of combustion and detonation. The corresponding thermodynamic cycle is close to the Humphrey cycle with combustion at constant volume. A ramjet with such a PDC is called pulse detonation engine (PDE).

There are many attempts in the literature to theoretically estimate the PDE specific impulse [31, 32]. It is believed that PDEs fueled by hydrogen or hydrocarbon fuel can possess very high fuel-based specific impulse of 5500 and 2500, respectively, in a wide range of flight Mach number from 0 to 4–5. However, these estimates are based on a number of simplifications – for a single cycle, for instantaneous detonation initiation in conditions at sea level, in the absence of the approach stream, within the one-dimensional approximation, etc. In our recent studies [33, 34] we have conducted a multi-dimensional numerical simulation of operation of a PDE with a mechanical valve for supersonic flight with Mach 3 at different altitudes (8 to 28 km above sea level), taking into account the finite-time DDT in hydrocarbon (propane)–air mixture and the integration of the PDC with PDE air intake and nozzle. It is shown that in these conditions a high-frequency (~50–80 Hz) cyclic operation of the PDE with the repeatable ignition of the combustible mixture by a weak ignition source (~0.1 J) and fast repeatable DDT is possible to organize. The specific impulse and specific fuel consumption for the PDE operating on a stoichiometric propane–air mixture in flight conditions at altitudes up to 26 km were respectively 1700–1800 s and 0.19–0.21 kg/(N·hour), which is very close to the same characteristics of the ideal ramjet on conventional combustion operating on fuel-lean hydrocarbon–air mixture with the equivalence ratio of 0.7 [35]. As for the PDE specific thrust, its calculated value under these conditions was higher by 18–38%, than that for a conventional ideal ramjet.

The objective of the work outlined in this Section is to prove the feasibility of cyclic PDE operation (in the layout with air intake and nozzle) for subsonic and supersonic flight with Mach number from 0.4 to 5.0 at different altitudes ranging from sea level up to 28 km

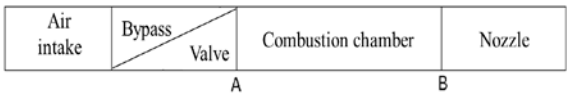

Fig. 8. Schematic of the PDE.

with all physical and chemical specific features of hydrocarbon fuel oxidation and combustion as well as the finite time of the turbulent flame acceleration and DDT taken into account.

Figure 8 is the schematic of an axisymmetric PDE consisting of the air intake, annular bypass channel, mechanical valve, PDC, and nozzle. We consider 5 different PDE configurations: for subsonic flight with Mach numbers of 0.4, 0.6, and 0.8 and for supersonic flight with Mach numbers of 3.0 and 5.0.

In an embodiment of the PDE for subsonic flight we use a subsonic air intake of small relative length and a Laval nozzle. As in [33, 34], the PDE has an annular bypass channel, providing a continuous flow of air through the air intake when the air supply to the PDC is closed by the mechanical valve. The PDC includes a section of fuel (propane gas) supply, a source of ignition (ignition energy of 0.1 J) and a set of specially shaped and positioned obstacles that provide fast DDT. In all cases, the PDE is designed to operate on a stoichiometric propane–air mixture with fuel-to-air equivalence ratio Φ=1.0. The fill factor of the PDC was taken to be χ = 0.9. The fill factor was defined as the ratio of the mass of fuel supplied to the PDC to the mass of fuel when the chamber is full (in Fig. 8: section A to B) with a stoichiometric mixture. The main dimensions of the PDE are: total length 1.3 m and diameter 82 mm.

In an embodiment of the PDE for supersonic flight we use a supersonic air intake with a central body providing the maximum pressure recovery at zero angle of attack and a Laval nozzle. The engine is also equipped with an annular bypass channel and a mechanical valve, and the PDC includes a section of fuel (propane gas) supply, a source of ignition (ignition energy of 0.1 J) and a set of specially shaped and positioned obstacles that provide fast DDT. The coefficients Φ and χ take the same values: Φ = 1 and χ = 0.9. The main dimensions of the PDE are: total length 2.2 m and diameter 82 mm.

As in [33, 34], the compressible turbulent reactive flow in the PDE was simulated numerically in a two-dimensional axisymmetric approximation. A mathematical model was based on the Unsteady Reynolds-Averaged Navier–Stokes (URANS) equations of conservation of mass, momentum and energy. Turbulent fluxes of matter, momentum, and energy were modeled by the k-ε turbulence model. Simulation of chemical sources in turbulent combustion, DDT, and detonation required modeling of frontal combustion, low-temperature preflame reactions and high-temperature volumetric reactions. For this purpose, we used the combined Flame Tracking – Particle (FTP) method [36], based on the simultaneous explicit tracking of the turbulent flame front and the semi-implicit calculation of preflame shock-induced

volumetric reactions by the Joint Velocity–Scalar Probability Density Function method [37].

The system of governing equations supplemented by the turbulence model and the combined FTP method was closed with the caloric and thermal equations of state of an ideal gas with variable specific heats, as well as with proper initial and boundary conditions. All thermo-physical parameters of the gas were considered temperature and pressure dependent. For the numerical solution, a method based on the finite volume discretization of the equations with the first-order approximation in space and time was used. In order to avoid excessive mesh refinement close to solid walls, a standard method of wall functions was applied.

To determine the PDE thrust performance, we calculated four or five operation cycles (to achieve a fully reproducible limit cycle) with the external flow around the engine. In all cases, both the pressure forces (the integral of the absolute pressure over all solid surfaces) and the viscous drag (integral of viscous shear stress over all solid surfaces) were calculated both in the inner and the outer streams. Special calculations on finer grids showed a negligible effect of grid size on the flow structure and the resultant thrust.

Table 1 shows the results of calculations for the flight Mach numbers M = 0.4, 0.6, 0.8, 3.0, and 5.0. Here, the following notations are adopted: Z is the flight altitude; f is the frequency of the operation process; F is the thrust (the vector sum of the effective thrust and aerodynamic drag force); I_{sp} is the fuel-based specific impulse; R_{sp} is the specific thrust (engine thrust per mass flow of air); C_{sp} is the specific fuel consumption (hourly fuel consumption attributable to the 1 N of thrust developed by the engine). To determine the thrust F developed by the PDE, it was necessary to calculate the vehicle drag force in flight conditions. This force was determined by solving the same problem with two changes: "with one misfire" (method 1), and "two misfires" (method 2). In the first case, the problem was first solved until fully reproducible limit cycle (four or five cycles) and in the subsequent cycle the combustible mixture was not ignited. In the second case, the problem was also solved to achieve a fully reproducible limit cycle (four to five cycles), and the next two cycles were calculated without ignition. The difference between the two methods of calculating the aerodynamic drag is due to the fact that in the first case, the combustible mixture filling the PDC displaces hot combustion products from the previous cycle, whereas in the second case the combustible mixture filling the PDC displaces unreacted (cold) fuel-air mixture from the previous cycle. In both cases, the drag force acting on the PDE in flight was determined by the last cycle in which ignition was absent. Table 1 shows two values of F, I_{sp}, R_{sp}, and C_{sp}: one obtained by method 1 (record without parentheses) and another by method 2 (parenthetical entry).

The most important result of this work is the proof of the potential of the high-frequency cyclic (40–75 Hz), pulse-detonation operation process in the PDE for subsonic flight with a Mach number of 0.4 to 0.8 and a supersonic flight with a Mach number of 3.0 and 5.0 with positive effective thrust (total force acting on the PDE). The specific impulse of the PDE for subsonic flight at low altitudes was shown to achieve 1200(1500) s. For supersonic flight with Mach numbers 3.0 and 5.0, the specific impulse was shown to reach 1600(1800) s at high flight altitudes up to 28 km. In contrast to the conventional ramjet, whose efficiency in subsonic flight is extremely low, the PDE in such a flight can work quite effectively. The same applies to the supersonic flight with Mach 5.0: according to [38], in such a flight a conventional ramjet has a relatively low specific impulse of 900–1200 s.

Figures 9a and 9b show the predicted time histories of the instantaneous effective thrust acting on all solid surfaces of the PDE in four to five operation cycles when flying with Mach 0.8 at an altitude of 500 m (Fig. 9a) and when flying with Mach 5.0 at an altitude of 28 km (Fig. 9b). As is seen, the average effective thrust is positive, i.e. the PDE has to move with acceleration. In both cases, there was a fast DDT in the combustion

Table 1

Results of calculations for PDE flight with Mach 0.4, 0.6, 0.8. 3.0, and 5.0 at different altitudes.

M	Z, km	f, Hz	F, N	I_{sp}, s	R_{sp}, kN/(kg/s)	Csp, kg/(N·hour
0.4	0	39	161(155)	1470 (1410)	0.92(0.88)	0.25(0.26)
0.6	0	57	225(200)	1580 (1410)	0.99(0.88)	0.23(0.26)
0.8	0	75	263(218)	1460(1190)	0.91(0.73)	0.25(0.3)
	5	70	144(115)	1460(1210)	0.91(0.74)	0.25(0.3)
	10	65	79(67)	1520(1280)	0.95(0.80)	0.24(0.29)
3.0	10	50	695.5(757.4)	1715 (1865)	1.09 (1.18)	0.21 (0.20)
	20	50	142.6(155.5)	1655 (1800)	1.05 (1.15)	0.22 (0.20)
	26	49	53.3(56.9)	1630 (1790)	1.02 (1.10)	0.22 (0.21)
5.0	28	55	33(37)	1640(1600)	1.03(1.01)	0.22(0.23)

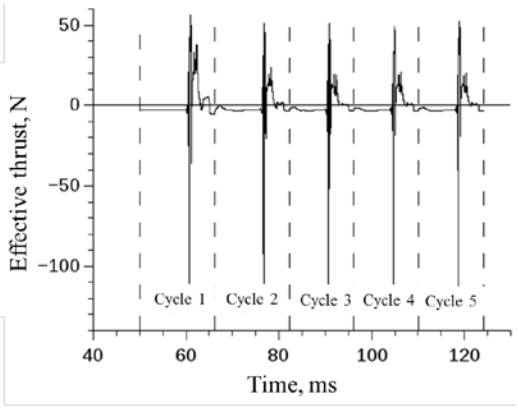

(a)

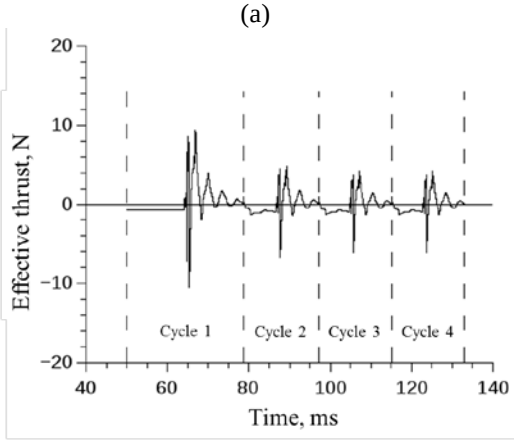

(b)

Fig. 9. Calculated time histories of the instantaneous effective thrust acting on all PDE solid surfaces in five operation cycles in flight with a Mach number 0.8 at 500 m (a) and in four cycles in flight with Mach 5.0 at 28 km altitude (b).

chamber resulting in the formation of retonation and detonation waves. The noise at the curves is explained by reflections of pressure waves from solid surfaces in the engine path, including the valve, shaped obstacles, and nozzle.

Thus, our calculations proved that in its potential the PDE is the unique type of ramjet propulsion system that could be used in both subsonic and supersonic aircraft.

3.5 Pressure Gain Rotating-Detonation Combustor

A rotating detonation combustor (RDC), first proposed by Voitsekhovsky in 1959 [39], is considered one of the most promising for further improving the aircraft propulsion units and power plants, in particular, gas turbine engines (GTE).

In the past decade, interest in the RDC concept increased significantly [40–46]. Reported in these papers are the results of experimental and computational studies of the process of operation of the RDC.

The specific objective of our work outlined in this Section is to show the feasibility of RDC integration in a GTE (Fig. 10), i.e. to prove the possibility of organizing the operation process in an annular combustion chamber with a wide gap, comparable to the height of the last stage of the compressor blades, with

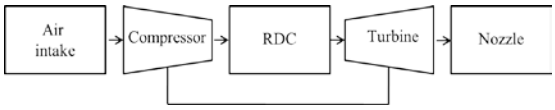

Fig. 10. Schematic of gas-turbine engine with RDC.

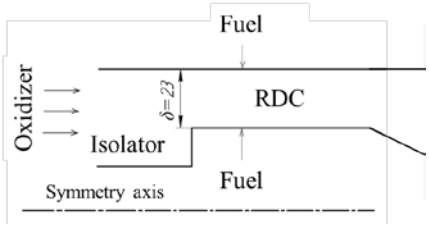

Fig. 11. Schematic of RDC with inlet isolator.

separate feeding of fuel and oxidizer. The main problem to be solved is to design an inlet isolator providing damping of pressure fluctuations for the last stage of the compressor in a GTE.

Figure 11 is a schematic of RDC annular gap of width δ = 23 mm with the corresponding inlet isolator. Oxidant (air) under pressure P_{in} = 9 atm at a temperature of 550 K is fed in through the inlet isolator axially. Fuel (hydrogen) is supplied from the fuel manifold through 80 radial injector bores: 40 in the outer wall and 40 in the inner wall. Pressure and temperature of hydrogen in the fuel manifold are kept constant and equal to 27 atm and 298 K. The outlet section of the RDC is the divergent nozzle composed from the central body in the shape of a cone; the nozzle is attached to the large receiver. Special calculations have shown that the conditions at the receiver boundaries do not affect the flow structure in the RDC. The mathematical formulation of the problem, the calculation method and the procedure for initiating detonation in the RDC were described in detail in [47, 48].

Initiation of detonation preceded by purging the RDC with fuel components. Figure 12 shows the successive distributions of hydrogen mass fraction in the RDC cross section located at an axial distance of 20 mm downstream from the hydrogen supply openings for first 30 μs of purging. It can be seen that in this section in about 20 μs after the start of purging the hydrogen–air mixture has a composition close to stoichiometric, but the mixture is periodically stratified: layers with fuel-rich and fuel-lean mixture are interspersed.

About 3–4 ms after the initiation of detonation the periodic operation mode with a single detonation wave propagating in the annular gap at the average velocity of 1950 m/s is established in the RDC. The rotation frequency of the detonation wave is approximately equal to 2 kHz. Figure 13 shows the calculated instantaneous static pressure (a) and temperature (b) distributions in the vicinity of the outer RDC wall in the periodic operation mode with a single detonation wave. It is seen that the hydrogen–air mixture ahead of the detonation wave is periodically stratified not only in terms of the composition (see Fig. 12), but also in terms of the temperature (Fig. 13b), as the air enters the inlet-

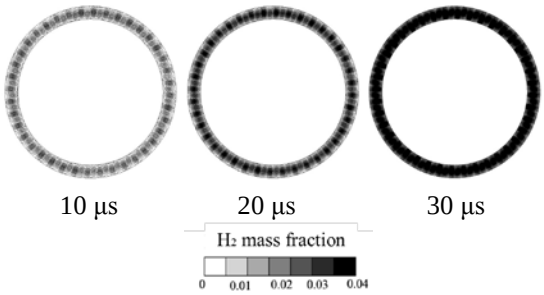

Fig. 12. Snapshots of hydrogen mass fraction in RDC during purging stage before ignition.

isolator with temperature 550 K and hydrogen, expanding into the injector holes, is cooled to a temperature of about 200 K. In addition to the periodic stratification of the mixture temperature and composition in the RDC cross sections, a substantial variation in the temperature and composition of the hydrogen–air mixture along the height of the circular layer in front of the detonation wave is observed. For this reason, a highly curved wave front, with its upper part running ahead of its lower part at a distance of about 2δ, and the front height is approximately 4,5δ (~ 100 mm).

For comparison, Fig. 14 shows the calculated instantaneous distributions of static pressure (a) and temperature (b) in the vicinity of the outer wall in a steady-state diffusion combustion (deflagration) in the same annular chamber. Deflagration is obtained by igniting the mixture evenly throughout the area over the holes of hydrogen supply. This combustion mode covers the entire cross section of the chamber, and the pressure and temperature decrease monotonically toward the nozzle.

Figure 15 shows the calculated time histories of the static pressure at two points: at a point located at a distance of 50 mm above the hydrogen supply holes (solid line) and at a point in the inlet isolator (dashed line) when operating in the detonation mode.

The most important result of this work is the proof that almost complete damping of pressure fluctuations can be achieved at the last stage of the compressor in the GTE equipped with an RDC if the inlet isolator of specific design is used. Indeed, the maximum deviation of the dashed curve from the straight line in Fig. 15 is only 3%P_{in}. In this example, the maximum average static pressure in the RDC is 8.6 atm. As for the total pressure, its calculated distribution in the detonation mode is shown in Fig. 16 by a solid curve. For comparison, the dashed curve shows the distribution of the total pressure in the same combustion chamber at a steady deflagration mode. It follows from Fig. 16 that unlike the deflagration mode in which the total pressure decreases along the axis of the chamber, the detonation mode exhibits the total pressure rise to 10.3 atm, i.e. 14-15% higher than P_{in}.

Thus, by means of numerical simulation we proved the possibility of organizing a cyclic operation of the

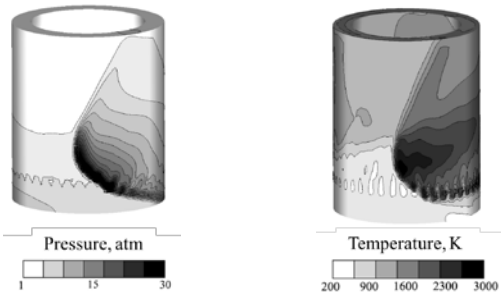

(a) (b)

Fig. 13. Snapshots of static pressure (a) and temperature (b) in the vicinity to the outer RDC wall in conditions of the periodic operation mode with a single detonation wave. Detonation propagates clockwise.

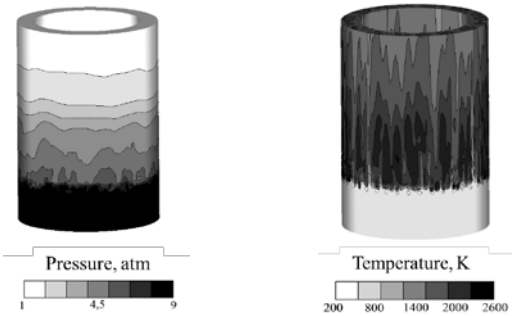

(a) (b)

Fig. 14. Snapshots of static pressure (a) and temperature (b) in the vicinity to the outer RDC wall in conditions of the steady-state diffusion combustion (deflagration).

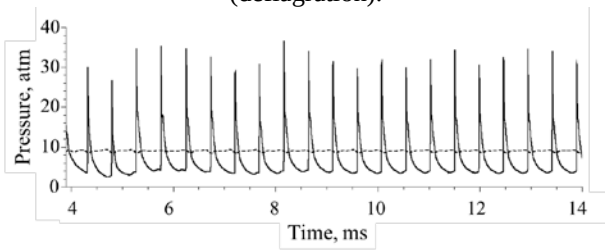

Fig. 15. Predicted time histories of static pressure in two locations: in the RDC (solid curve) and in the inlet isolator (dashed curve).

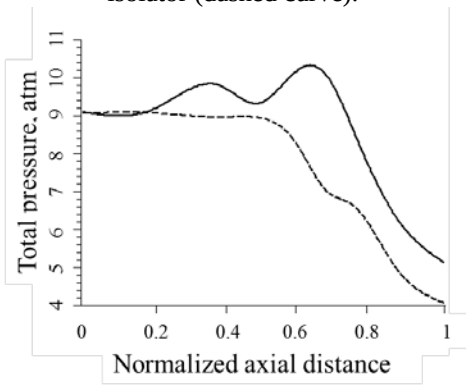

Fig. 16. Predicted distributions of the averaged total pressure along the RDC axis in the detonation (solid curve) and deflagration (dashed curve) operation modes.

annular RDC with separate supply of fuel and oxidizer and a wide annular gap comparable to the height of the blades of the last compressor stage in a GTE. The inlet isolator of specific design attached to the RDC from the upstream was shown to ensure almost complete damping of pressure fluctuations at the GTE compressor. A 15-percent total pressure gain was shown to be attained in the RDC.

4. Conclusions

Physical principles and problems of controlling DDT and detonation propagation in gaseous and two-phase systems are outlined. Several examples of the potential use of controlled fast DDT and detonation propagation in different devices of interest for energy and propulsion sectors are discussed, namely (1) the PDB operating on natural gas–air mixture, (2) the micro-PDRE for orbit correction, (3) the air-breathing PDE integrated in subsonic and supersonic ramjets, and (4) the pressure gain RDC designed to replace a conventional combustor in a GTE.

Acknowledgements

Valuable contribution of Aksenov V.S., Avdeev K.A., Basevich V. Ya., Borisov A.A., Dubrovskii A.V., Frolov F.S., Gusev P.A., Ivanov V.S., Koval A.S., Medvedev S.N., Shamhin I.O., Smetanyuk V.A., and Zangiev A.E. of the Center for Pulse-Detonation Combustion at Semenov Institute of Chemical Physics to this work at its different stages is gratefully acknowledged. This work was partly supported by the Ministry of Education and Science of the Russian Federation (State contract No. 16.526.12.6018 "Development of energy-efficient high-speed pulse-detonation gas burner to improve thermal performance of industrial furnaces and thermal power plants").

References

[1] W. A. Bone, R. P. Fraser, Philos. Trans. R. Soc. London, Ser. A 228 (1929) 197.

[2] Ya. B. Zel'dovich, Theory of Combustion and Detonation of Gases, Akad. Nauk SSSR Publ., Moscow, 1944.

[3] K. I. Shchelkin, Fast Combustion and Spin Detonation of Gases, Voenizdat Publ., Moscow, 1949.

[4] A. K. Oppenheim, Introduction to Gasdynamics of Explosions, Springer, Wien, 1972.

[5] A. J. Higgins, P. Pinard, A. K. Yoshinaka, and J. H. S. Lee, in: Pulse Detonation Engines, S. M. Frolov, ed., Torus Press, Moscow, 2006, 65–86.

[6] S. M. Frolov, V. Ya. Basevich, V. S. Aksenov, and S. A. Polikhov, J. Propulsion Power 19 (4) (2003) 573.

[7] S. M. Frolov, V. Ya. Basevich, V. S. Aksenov, and S. A. Polikhov, Dokl. Phys. Chem. 394 (1) (2004) 16.

[8] S. M. Frolov, V. Ya. Basevich, V. S. Aksenov, and S. A. Polikhov, Khim. Fiz. 23 (4) (2004) 61.

[9] S. M. Frolov, V. Ya. Basevich, V. S. Aksenov, and S. A. Polikhov, Dokl. Phys. Chem. 394 (2) (2004) 39.

[10] S. M. Frolov, V. Ya. Basevich, V. S. Aksenov, and S. A. Polikhov, J. Propulsion Power 21 (1) (2005) 54.

[11] S. M. Frolov, J. Loss Prevention 19 (2–3) (2005) 238.

[12] S. M. Frolov, J. Propulsion Power, 6 (2006) 1162.

[13] S. M. Frolov, V. Ya. Basevich, and V. S. Aksenov, Shock Waves 14 (3) (2005) 175.

[14] V. Ya. Basevich, S. M. Frolov, and V. S. Posvyanskii, Khim. Fiz. 24 (7) (2005) 58.

[15] S. M. Frolov, Rus. J. Phys. Chem. B, 2(3) (2008) 442–455.

[16] O. Peraldi, R. Knystautas, and J. H. S. Lee, Proc. Combust. Inst. 21 (1986) 1629.

[17] M. Kuznetsov, G. Ciccarelli, S. Dorofeev, V. Alekseev, Yu. Yankin, N. H. Kim, Shock Waves, 12 (2002) 215–220.

[18] M. Kuznetsov, V. Alekseev, I. Matsukov, T. H. Kim, Proc. 8th Symp. (Int.) on Hazards, Prevention and Mitigation of Industrial Explosions (SHPMIE), Jokohama, Japan, 2010, Paper No. ISH_118.

[19] A. A. Vasil'ev, in: Confined Detonations and Pulse Detonation Engines, ed. G. Roy, S. Frolov, R. Santoro, and S. M. Tsyganov, Torus Press, Moscow, 2003, 41–48.

[20] S. M. Frolov, V. S. Aksenov, A. A. Skripnik, Dokl. Phys. Chem., 436(1) (2011) 10–14.

[21] S.M. Frolov, V.S. Aksenov, V.S. Ivanov, S.N. Medvedev, V.A. Smetanyuk, K.A. Avdeev, and F. S. Frolov, Rus. J. Phys. Chem. B, 5(4) (2011) 625–627.

[22] S. M. Frolov, V. Ya. Basevich, V. S. Aksenov, P. A. Gusev, V. S. Ivanov, S. N. Medvedev, V. A. Smetanyuk, K. A. Avdeev, F. S. Frolov, Rus. J. Phys. Chem. B, 5(4) (2011) 661–663.

[23] S. M. Frolov, V. S. Aksenov, A. A. Berlin, Rus. Fed. Patent Appl. for "The Technique of Detonation Initiation in a Tube with Combustible Mixture and the Device for its Implementation," No. 2427756, filed 27 Aug. 2011.

[24] S. M. Frolov, V. S. Aksenov, A. A. Berlin, Rus. Fed. Patent Application for "The Device for Detonation Initiation," No. 2430303, filed 27 Nov. 2011.

[25] S. M. Frolov, V. S. Aksenov, A. A. Berlin, Rus. Fed. Patent Application for "The Technique of Detonation Initiation in a Tube with Combustible Mixture and the Device for its Implementation," No. 2429409, filed 20 Sep. 2011.

[26] S. M. Frolov, V. S. Aksenov, V. S. Ivanov, Rus. J. Phys. Chem. B, 5(4) (2011) 664–667.

[27] Ya. B. Zel'dovich, J. Exp. Theor. Phys. 10(5) (1940) 543–568.

[28] S. M. Frolov, V. S. Aksenov, Dokl. Phys. Chem., 427(1) (2009) 129–132.

[29] I. V. Semenov, P. S. Utkin, V. V. Markov, S. M. Frolov, V. S. Aksenov, Comb. Sci. Techn., 182(11) (2010) 1735-1746.

[30] S. M. Frolov, I. O. Shamshin, S. N. Medvedev, A. V. Dubrovskii, Dokl. Phys. Chem., 438(2) (2011) 114-117.

[31] K. Kailasanath, AIAA J., 41(2) (2003) 145–159.

[32] G. D. Roy, S. M. Frolov, A. A. Borisov, D. Netzer, Progr. Energy Comb. Sci., 30(6) (2004) 545-672.

[33] V. S. Ivanov, S. M., Rus. J. Phys. Chem. B, 5(4) (2011) 597–609.
[34] A. E. Zangiev, V. S. Ivanov, S. M. Frolov, Rus. J. Phys. Chem. B, 7(5) (2013) 165.
[35] J. Kurzke, in: RTO-AVT-VKI Lecture Series 2010-AVT 185, Von Karman Inst. Fluid Dynamics, September 13–15 (2010) 2.1–2.33.
[36] S. M. Frolov, V. S. Ivanov, in: Progress in propulsion physics, L. DeLuca, C. Bonnal, O. Haidn, and S. Frolov eds. EUCASS Advances in Aerospace Sciences Book Ser. EDP Sciences, TORUS PRESS, 2 (2011) 533-554.
[37] S. B. Pope, Proc. Comb. Inst., 23 (1990) 120.
[38] J.-L. Moerel, W. Halswijk, in: RTO-AVT-VKI Lecture series 2010-AVT 185, Von Karman Inst. Fluid Dynamics. September 13–15 (2010) 27.
[39] B. V. Voitsekhovskii, Dokl. Akad. Nauk SSSR 129 (1959) 1254.
[40] F. A. Bykovskii, S. A. Zhdan, E. F. Vedernikov, Combust. Explos., Shock Waves, 45 (2009) 606.
[41] D. M. Davidenko, I. Gokalp, A. N. Kudryavtsev, in: Deflagrative and Detonative Combustion, G. D. Roy and S. M. Frolov, eds, Torus Press, Moscow, 2010, 27.
[42] D. M. Davidenko, I. Gokalp, A. N. Kudryavtsev, AIAA Paper No. 2008-2680 (2008).
[43] J. Kindracki, P. Wolanski, Z. Gut, Shock Waves, 21(2) (2011) 75.
[44] D. A. Schwer and K. Kailasanath, Proc. Combust. Inst. 33 (2010).
[45] M. Hishida, T. Fujiwara, P. Wolanski, Shock Waves, 19 (1) (2009) 1.
[46] Y.-T. Shao, M. Liu, J.-P. Wang, Combust. Sci. Techn., 182 (2010)1586.
[47] S. M. Frolov, A. V. Dubrovskii, V. S. Ivanov, Rus. J. Phys. Chem. B, 6(2) (2012) 276–288.
[48] S. M. Frolov, A. V. Dubrovskii, V. S. Ivanov, Rus. J. Phys. Chem. B, 7(1) (2013)35–43.